

## Impact of ionizing radiation doses on nanocrystalline TiO<sub>2</sub> layer in DSSC's photoanode film



M. Khalid Hossain<sup>a,\*</sup>, M.T. Rahman<sup>b,1</sup>, M.K. Basher<sup>a</sup>, M.J. Afzal<sup>c</sup>, M.S. Bashar<sup>d</sup>

<sup>a</sup> Institute of Electronics, Atomic Energy Research Establishment, Bangladesh Atomic Energy Commission, Dhaka 1349, Bangladesh

<sup>b</sup> Dept of Materials Science & Engineering, University of Rajshahi, Rajshahi 6205, Bangladesh

<sup>c</sup> Dept of Physics, The University of Lahore, Lahore 54000, Pakistan

<sup>d</sup> Institute of Fuel Research and Development, Bangladesh Council of Scientific and Industrial Research, Dhaka 1205, Bangladesh

### ARTICLE INFO

#### Keywords:

Effect of ionizing radiation  
Structural properties  
Optical properties  
DSSC photoanode film  
Nanocrystalline TiO<sub>2</sub>  
Dye-sensitized solar cell

### ABSTRACT

In dye-sensitized solar cell (DSSC) properties of nanocrystalline oxide layer of photoanode may changes when exposed to ionization radiation environment which may leads to change the cell performance. In this study, 10 μm thick TiO<sub>2</sub> (Degussa-P25) was deposited as a photoanode film on microscopic glass slide with the doctor-blade coating. The deposited film was subjected to different gamma (γ) radiation doses (0–20 kGy) to study the effect of ionizing radiation on morphological, structural, optical and compositional characteristics of the film. At 10 kGy dose, dislocation density (DD), strain, crystallites per unit surface area (CPSA), specific surface area (SSA) of anatase phase (1 0 1) of the film were decreased abruptly, conversely, crystal size and morphology index (MI) were increased at the same radiation dose slowly. UV-Vis-NIR spectroscopy results showed that in irradiated photoanode film the light transmittance and absorption depth were decreased, whereas, absorption and absorption coefficient were increased beyond the visible wavelength. The optical band gap of the irradiated film was increased by 12.5% when the gamma radiation dose increased from 0 kGy to 20 kGy. Thus, the irradiation induced changes in physio-chemical properties of nanocrystalline photoanode film may affect the DSSC cell performance.

### Introduction

Over the years, among various types of solar cell the dye-sensitized solar cell has become point of interest to many researchers [1–5]. The cell performance of dye sensitized solar cell (DSSC) greatly depends on photoanode materials properties, types of the dye sensitizer and their adsorption properties [5–8]. Specially, nanocrystalline thin oxide layer (photoanode's nanocrystalline film) such as mesoporous TiO<sub>2</sub> layer provides high specific surface area and high dye adsorption properties resulting in better cell performance [7,9]. Nanocrystalline TiO<sub>2</sub> layer reduces the electron-hole recombination by providing a straight moving path for electrons to flow [10–12]. However, the properties of oxide layer become vulnerable to several damages or changes [13,14] during their function under radiation-exposed location like space, place close to radiation establishment etc. resulting device degradation and failure. DSSC is expected to become a potential device to mitigate the demand of electrical energy, both in space craft and industries. Therefore, evaluation of radiation effect on nanocrystalline oxide layer of DSSC is

very important.

In DSSC, titanium dioxide has been applied as an electron transport layer because of its high performance, low cost, chemical inertness, thermal and photo-stability [15]. Degussa P25 TiO<sub>2</sub> nanopowder have already gained popularity due to improved synergic effect [16] and significant advantages of mixed anatase and rutile phase [17–19]. Amongst other influencing factors [6–8], several properties of photoanode film such as crystal structure, specific surface ratio, grain size, traps, defects, surface morphology, photocatalytic activity, optical absorbance, reflectance, transmittance, absorption depth, absorption coefficient and optical bandgap, etc. have remarkable influence on photovoltaic performance of DSSC [7,17,20].

It is important to note that alteration of physical, optical and electrical properties occurs due to exposure to ionization radiation, such as gamma radiation [21–24]. In previous studies, Date et al. reported gamma irradiation induced conductivity in insulators [25], Banerjee et al. examined the effect on crystal structure of TiO<sub>2</sub> [26], Samet et al. assessed the effect on optical, structural and radiocatalytic properties of

\* Corresponding author.

E-mail address: [khalid.baec@gmail.com](mailto:khalid.baec@gmail.com) (M.K. Hossain).

<sup>1</sup> Authors contributed equally to this work.

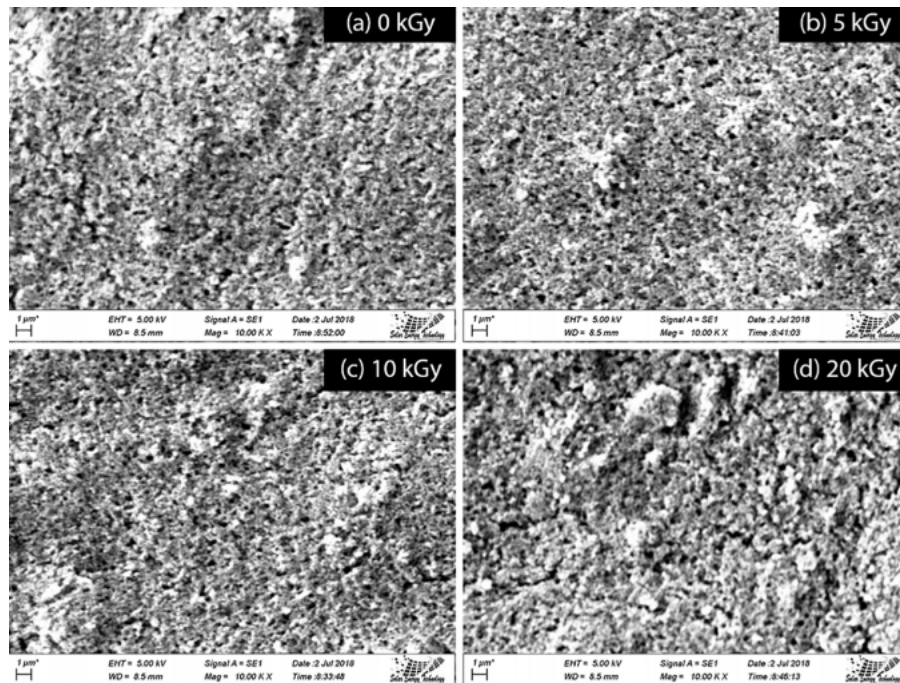


Fig. 1. SEM images of  $\text{TiO}_2$  film at various gamma doses (a) 0 kGy, (b) 5 kGy, (c) 10 kGy, and (d) 20 kGy.

Cu-incorporated  $\text{TiO}_2$  nano-particles [27], Reyhani et al. reported the changes in optical and structural properties of ZnO nanowires [28], Wang et al. explored the changes in optical and structural properties of cerium/titanium-doped oxyfluoride [29], Ali et al. studied the effects on electrical, optical and structural properties of n- $\text{TiO}_2$ /p-Si heterojunction [30], Khalouie et al. investigated influence on surface and reflection quality of silver mirror [31], Jovanovic et al. reported the hydrolytic and thermal stability of  $\text{TiO}_2$  based nanocomposite [32], Lamo et al. studied influence of photocatalytic behavior of  $\text{TiO}_2$  due to gamma radiation [33]. However, the ionizing radiation effect on DSSC photoanode film is still unexplored and the purpose of this current investigation is to clarify the consequence of  $\gamma$ -radiation on nanocrystalline  $\text{TiO}_2$  layer used for dye-sensitized solar cell photoanode applications.

In this paper,  $\text{TiO}_2$  paste was prepared with unique chemical combination [7,9,34] and deposited on glass substrate using doctor blade method. The deposited nanocrystalline oxide film was then subjected to gamma radiation doses varying from 0 kGy to 20 kGy. Later, effects of irradiation on structure, morphology, composition and optical characteristics were analyzed by XRD, surface profiler, SEM, EDS and UV-Vis spectroscopy.

## Materials and methods

### Materials

$\text{TiO}_2$  nanopowder (Degussa P25, USA), citric acid ( $\text{C}_6\text{H}_8\text{O}_7$ ), PEG, microscopic glass substrate, Triton X-100 were the materials used in this study.

### $\text{TiO}_2$ photoanode film coating

In a clean and dry beaker, Titanium dioxide nanopowder (1.0 g), citric acid (0.1 M, 1 mL), non-ionic surfactant triton X-100 (0.05 mL), and polyethylene glycol (0.1 mL) were mixed well to form  $\text{TiO}_2$  paste.

The paste was then sonicated for 20 min to ensure proper mixing of the constituents using ultrasonic bath. Five glass substrates

(0.5 cm  $\times$  0.5 cm) were cleaned with distilled water to remove any unwanted adherent from the surface and dried in an oven. Then, with the help of doctor blade method 10  $\mu\text{m}$  thick  $\text{TiO}_2$  layer was developed on the glass substrate using the prepared paste [6]. The  $\text{TiO}_2$  film thickness was measured with the help of stylus surface profiler (Dektak 150, Veeco, USA). Finally, the substrates were annealed for 1 h at 450  $^\circ\text{C}$  as well as cooled very slowly to avoid the cracking of the photoanode film layer.

### Gamma irradiation

Every fabricated samples were irradiated using batch type Cobalt-60 gamma source with source activity 55.67 kCi, at Institute of Food and Radiation Biology (IFRB), Bangladesh Atomic Energy Commission [35]. All the samples were kept about 7.62 cm away from the source as well as at right angle with the source. The dosage rate of the gamma radiation source was found 7.6 kGy/h. The absorbed doses were measured using liquid phase dosimetry setup (Ceric-cerous). The samples were irradiated for 8, 39, 79, 118, and 158 min to get 1, 5, 10, 15, and 20 kilo Gray absorbed  $\gamma$ -doses.

### Characterization

The XRD patterns of both irradiated and unirradiated specimens were obtained using X-ray diffractometer ( $\lambda = 1.5406 \text{ \AA}$ ). The scan was conceded with a step size of 0.02 $^\circ$  and a step time of 0.2 s.

The SEM image of both irradiated and unirradiated samples were taken to investigate particle size and surface morphology using Field Emission Scanning Electron Microscope (JEOL JSM-7600F, Tokyo, Japan). To eliminate charging effect the accelerating voltage was maintained at 5–7 kV. During SEM investigation EDS spectra was also taken at the same condition.

The UV-Vis spectra were taken to investigate optical properties of both irradiated and unirradiated samples with an UV-Visible spectrophotometer (Hitachi 4200, Japan).

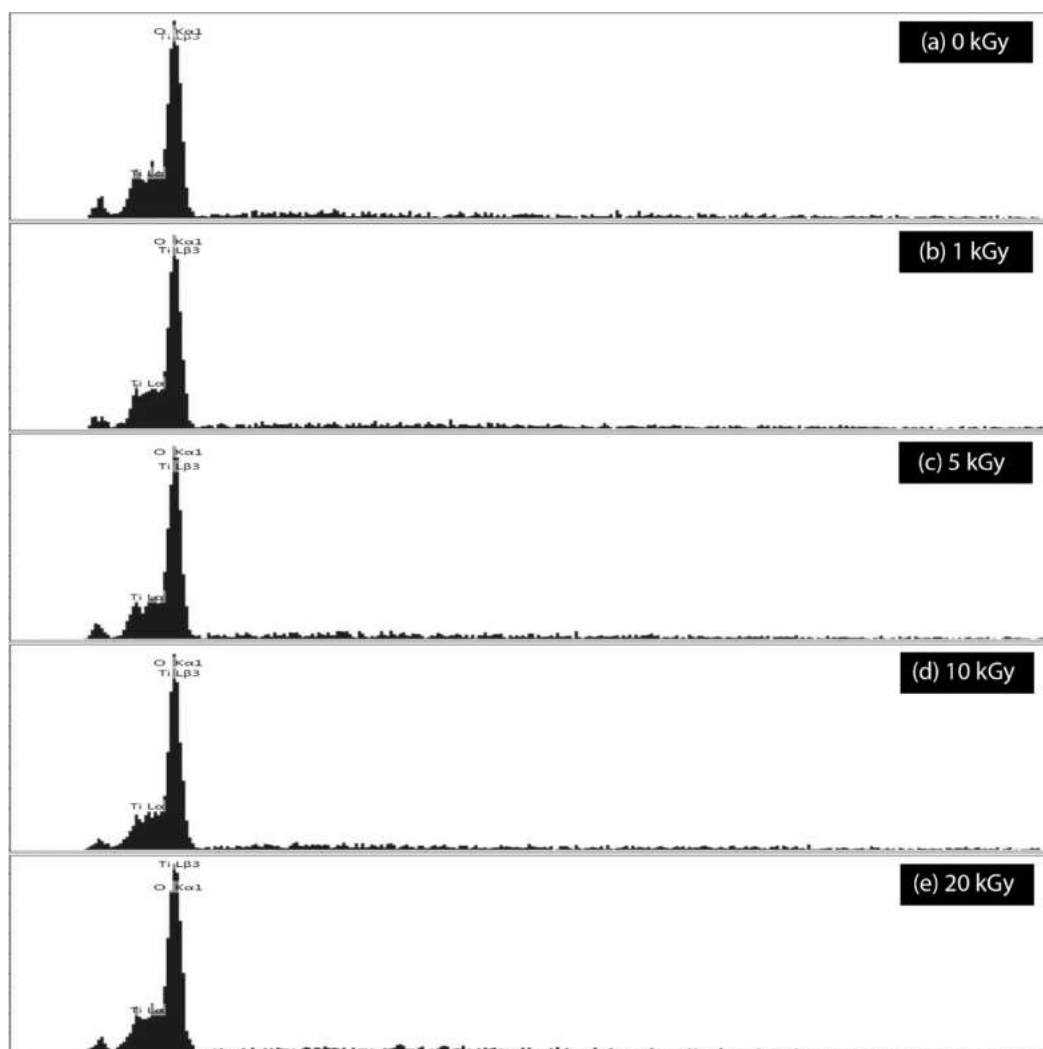


Fig. 2. EDS spectra of photoanodic  $\text{TiO}_2$  layer of DSSC at different gamma radiation doses.

## Results and discussion

### SEM analysis

Fig. 1 shows the SEM images of both unirradiated and irradiated nanocrystalline  $\text{TiO}_2$  film of photoanode. According to the figure, almost uniform layer of  $\text{TiO}_2$  nanoparticles were seen on the glass substrate prior to gamma irradiation. When the film is irradiated with 1–20 kGy gamma radiation doses both lattices distortions and reduction in grain size of the  $\text{TiO}_2$  nanoparticles were occurred. This leads to further agglomeration of nanoparticles in different shapes. Therefore, roughness was increased in those irradiated films. The roughest surface was found for the sample irradiated with 20 kGy dose. This phenomenon ultimately influenced the optical properties of the photoanodic film.

### EDS analysis

Fig. 2 shows the EDS spectrum of both unirradiated and irradiated nanocrystalline  $\text{TiO}_2$  layer of photoanode as well as Table 1 represents the experimental data. According to the Fig. 2, the peaks found at 0.452 keV and 0.525 kilo electron volts confirms the presence of titanium and oxygen atom respectively. According to the table it is seen that both mass percentage and atomic percentages of Titanium were decreased by upsurge of gamma radiation doses. Conversely, mass

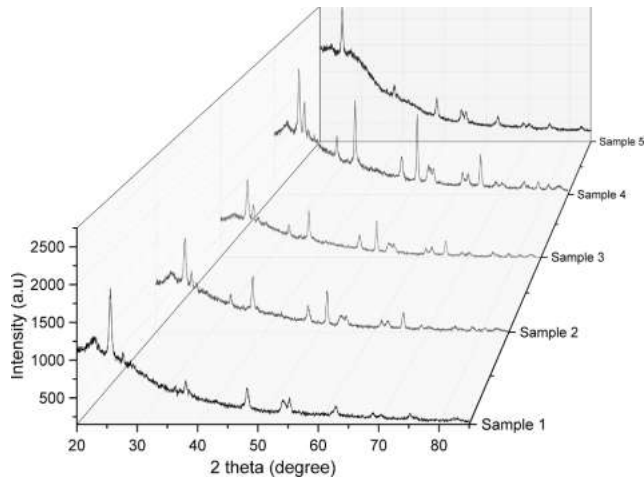
percentage and atomic percentages of Oxygen were increased with the increase of gamma radiation doses. The average atomic mass percentage was found 64.88% and 35.12% for Ti and O respectively in  $\text{TiO}_2$  film similar to the standard values of Ti (59.93%) and O (40.07%) in  $\text{TiO}_2$  compound. Additionally, the average atomic percentage was found 38.18% and 61.82% for Ti and O respectively.

### XRD investigation

Fig. 3 depicts the XRD patterns for different gamma radiation doses of  $\text{TiO}_2$  thin films deposited on glass substrate. All peaks observed from XRD patterns can be well indexed to the JCPDS card no. 00-021-1272 and JCPDS card no. 00-021-1276 confirming the presence of anatase phase and rutile phase of Titanium dioxide correspondingly. It is seen that the deposited thin film contains both anatase and rutile phases. With the reference of the figure it can be seen that intensity of the peaks increased upto 10 kGy then decreased at higher radiation dose. The obtained numerical data for FWHM and size of crystallite of anatase phase as well as rutile phase are tabulated in Tables 2 and 3 respectively. The FWHM value for the predominant peak (1 0 1) of anatase phase increased upto 5 kGy and thereafter decreased beyond this radiation dose. The crystallite size decreased upto 5 kGy and increased with increase of gamma radiation dose. Besides, the FWHM value for the predominant peak (1 1 0) of rutile phase increased with the increment of radiation doses, whereas, crystallite size decreased due to

**Table 1**Comparison of mass and atomic percentage of titanium (Ti) and oxygen (O) in TiO<sub>2</sub> film obtained from EDS spectra.

Element	Mass [%]						Atom [%]					
	Sample 1 (0 kGy)	Sample 2 (1 kGy)	Sample 3 (5 kGy)	Sample 4 (10 kGy)	Sample 5 (20 kGy)	Average	Sample 1 (0 kGy)	Sample 2 (1 kGy)	Sample 3 (5 kGy)	Sample 4 (10 kGy)	Sample 5 (20 kGy)	Average
Titanium (Ti)	67.3	64.7	63.5	63.4	65.5	64.88	40.7	38.0	36.8	36.6	38.8	38.18
Oxygen (O)	32.7	35.3	36.5	36.6	34.5	35.12	59.3	62.0	63.2	63.4	61.2	61.82

**Fig. 3.** XRD spectra of photoanodic TiO<sub>2</sub> layer of DSSC at different gamma radiation doses.

higher radiation doses. Most importantly, due to gamma irradiation (2 1 0) picks for rutile disappeared in all samples.

#### Gamma irradiation effect on mole fraction (MF) and phase content (PC)

Fig. 4 shows the influence of different radiation doses on MF and PC of both phases of thin film of Titanium dioxide. The XRD peak intensity of anatase (1 0 1) to rutile (1 1 0) was considered to calculate the molar ratio of both phases by following Spurr and Myers technique with the following expressions [6]:

$$W_R = 1/[1 + 0.8(I_A/I_R)] \quad (1)$$

$$W_A = 1 - W_R \quad (2)$$

where,  $W_A$  and  $W_R$  represents the mole fractions of anatase and rutile respectively;  $I_A$  and  $I_R$  represents the peak intensities of anatase and

rutile phases respectively.

According to the Fig. 4 it is seen that before gamma irradiation (0 kGy) of the TiO<sub>2</sub> film the mole fraction of anatase and rutile phase was found 58.45% and 41.54% respectively. With the increase of gamma dose such as 5 kGy and 10 kGy the mole fraction of anatase was increased, while decreased for rutile. Due to further increase of gamma radiation dose at 20 kGy the mole fraction of anatase phase decreased sharply to 52.90% and the mole fraction of rutile phase increased sharply to 47.09% respectively.

The phase contents of both anatase and rutile was changed in the same fashion as mole fraction as described above. Before irradiation of the sample, the phase content of anatase and rutile was found 60.91% and 39.08% respectively in the TiO<sub>2</sub> thin film. With increased gamma radiation dose such as 5 kGy and 10 kGy the phase content of anatase was increased, and decreased for rutile. Due to further increase of radiation dose at 20 kGy the phase content of anatase decreased to 55.43% but for rutile the value increased to 44.56%.

It is clear that no appreciable change in mole fraction was seen for both anatase and rutile phase up to 10 kGy radiation dose but the value changed drastically beyond this radiation dose. Similarly, no appreciable change in mole fraction was seen for both anatase and rutile phase up to 10 kGy radiation dose but the value decreased drastically beyond this radiation dose. Degussa P25 is used for its unique composition of anatase and rutile phase which gives better cell performance. The change of anatase and rutile phase due to gamma irradiation leads to change in cell performance of DSSC. Therefore, the gamma radiation dose higher than 10 kGy is crucial for altering the cell functioning of DSSC when exposed to radiation source or environment.

#### Gamma irradiation effect on crystallite size and strain

Fig. 5 shows the consequence with different radiation doses on crystallite size and strain of both phases of Titanium dioxide photoanode film.

Crystallite size ( $L$ ) was calculated by the using Debye-Scherrer formula [6,36–38]:

**Table 2**

Crystallite size and FWHM of anatase (A) phase at different gamma radiation doses.

Phase (Anatase)	Sample 1 (0 kGy)		Sample 2 (1 kGy)		Sample 3 (5 kGy)		Sample 4 (10 kGy)		Sample 5 (20 kGy)	
	FWHM	L [nm]	FWHM	L [nm]	FWHM	L [nm]	FWHM	L [nm]	FWHM	L [nm]
A (1 0 1)	0.442	18	0.467	17	0.477	17	0.427	19	0.429	19
A (1 0 3)	0.263	32	0.174	48	0.250	33	0.098	86	0.449	19
A (0 0 4)	0.415	20	0.386	22	0.413	20	0.379	22	0.476	18
A (1 1 2)	0.208	40	0.092	91	0.166	51	0.133	63	0.086	98
A (2 0 0)	0.537	16	0.531	16	0.575	15	0.527	17	0.569	15
A (1 0 5)	0.643	14	0.846	11	0.826	11	0.238	37	0.423	21
A (2 2 1)	0.338	27	0.442	20	0.531	17	0.406	22	0.492	18
A (2 1 3)	–	–	0.402	23	0.323	29	0.405	23	–	–
A (2 0 4)	0.692	13	0.571	16	0.527	18	0.496	19	0.529	18
A (1 1 6)	0.715	13	0.507	19	0.496	19	0.601	16	0.493	20
A (2 2 0)	0.441	22	0.428	23	0.107	91	0.504	19	0.473	21
A (2 1 5)	1.074	9	0.493	20	0.751	13	0.638	16	0.683	15
A (3 1 0)	–	–	–	–	0.245	41	0.207	49	0.114	88
A (2 2 4)	0.172	61	0.967	11	0.909	12	1.167	9	0.649	16

**Table 3**  
Crystallite size and FWHM of rutile (R) phase at different gamma radiation doses.

Phase (Anatase)	Sample 1 (0 kGy)		Sample 2 (1 kGy)		Sample 3 (5 kGy)		Sample 4 (10 kGy)		Sample 5 (20 kGy)	
	FWHM	L [nm]	FWHM	L [nm]	FWHM	L [nm]	FWHM	L [nm]	FWHM	L [nm]
R (110)	0.257	32	0.206	40	0.464	18	0.467	18	0.332	25
R (101)	0.558	15	0.393	21	0.503	17	0.263	32	–	–
R (200)	–	–	–	–	–	–	0.089	95	0.225	37
R (111)	0.135	63	–	–	0.325	26	0.136	62	0.344	25
R (210)	0.232	37	0.365	23	–	–	–	–	–	–
R (211)	0.091	98	0.141	63	0.207	43	0.427	21	–	–
R (220)	0.215	42	–	–	0.138	65	0.225	40	0.226	40
R (310)	–	–	0.103	91	–	–	–	–	0.161	58

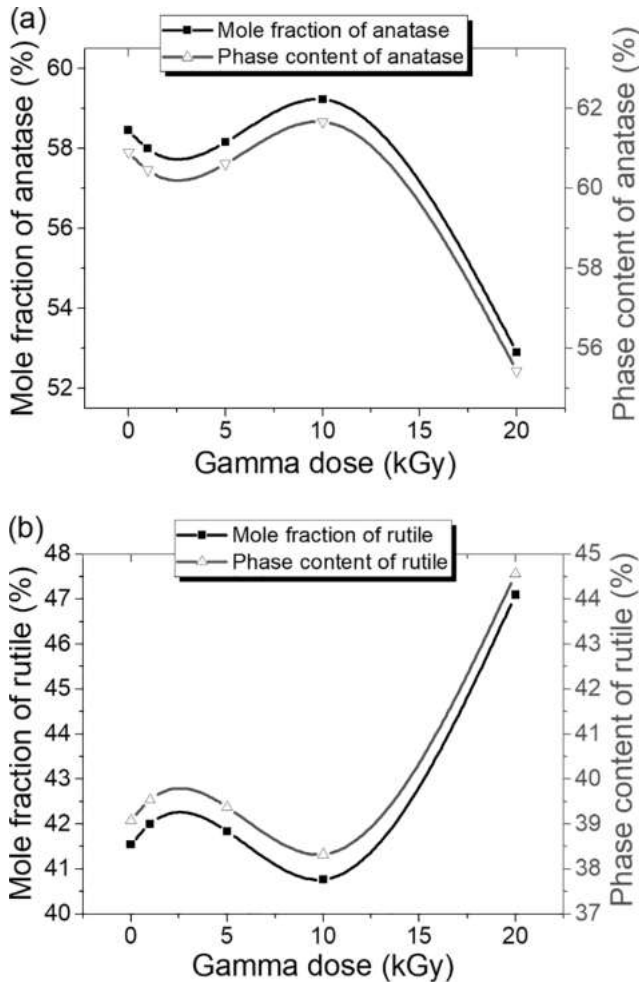


**Fig. 4.** Gamma doses effect on mole fraction and phase content of (a) anatase (101) and (b) rutile (110) phase of TiO<sub>2</sub> (Degussa-P25) based DSSC photoanode film.

$$L = \frac{K\lambda}{\beta \cos\theta} \quad (3)$$

Also, lattice strain (e) was calculated by following Williamson–Hall method [39] using the following formula [5]:

$$e = \frac{\beta}{4 \tan \theta} \quad (4)$$

where,  $\beta$  represents the full width at half-maximum (FWHM),  $K$  is a constant taken as 0.9,  $\lambda$  represents the wavelength of X-ray,  $\theta$  represents the Bragg's angle in degree.

According to the Fig. 5 it is seen that before gamma irradiation

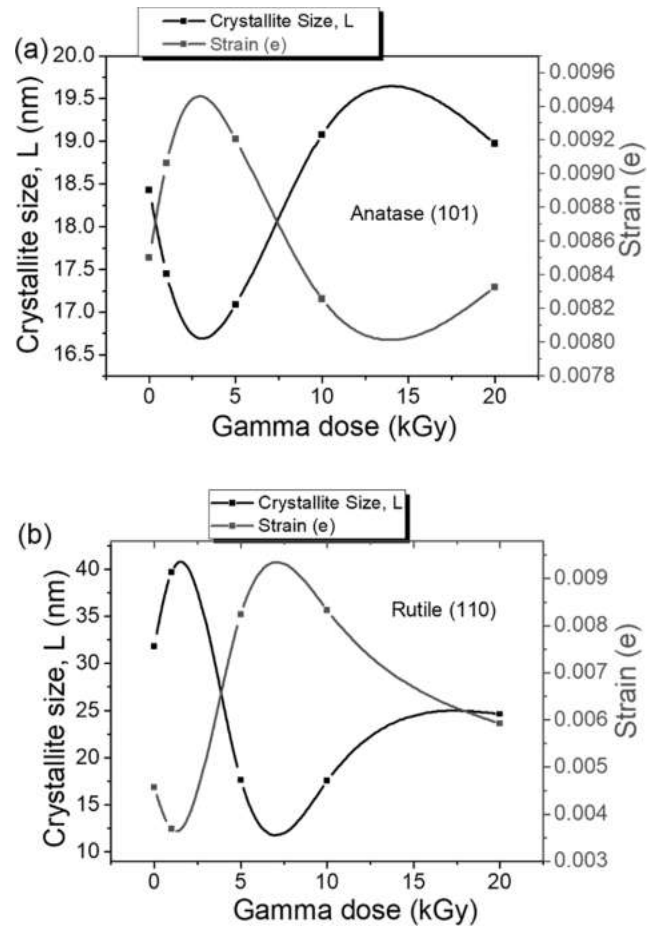


**Fig. 5.** Gamma doses effect on crystal size and strain of (a) anatase (101), and (b) rutile (110) phase of TiO<sub>2</sub> (Degussa-P25) based DSSC photoanode film.

(0 kGy) of the TiO<sub>2</sub> film the crystallite size of anatase and rutile phase was found 18.42 nm and 31.83 nm respectively. The crystallite size of anatase was decreased at lower gamma radiation doses (1 and 5 kGy) but increased at higher doses (10 and 15 kGy). Besides, for rutile the crystallite size was reduced with the increase of radiation doses such as 5, 10, and 20 kGy. Due to change in crystalline size of nanocrystalline mesoporous TiO<sub>2</sub> the pore size also reduces. Because of this reduced pore size total dye absorption amount will decrease, therefore, lower carrier electron will generate resulting lower performance of the solar cell.

The strain of rutile and anatase phases was found 0.0045e and 0.0085e respectively before gamma irradiation of the thin film. The strain of anatase was increased at lower gamma radiation doses such as 1 and 5 kGy but decreased at higher doses such as 10 and 15 kGy. Besides, the strain was increased for rutile with the increase of radiation

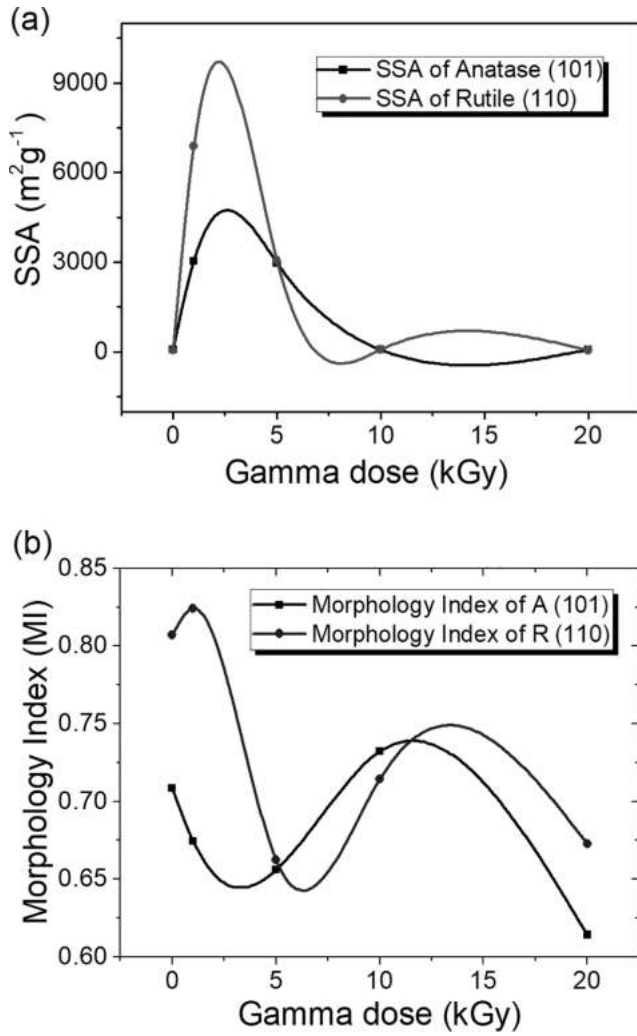


Fig. 6. Effect of gamma doses on (a) specific surface area (SSA), and (b) morphology index (MI) of anatase (101) and rutile (110) phase of TiO<sub>2</sub> (Degussa-P25) based DSSC photoanode film.

doses such as 5, 10, and 20 kGy.

Effect of gamma irradiation on SSA and MI

Fig. 6 shows consequence of different radiation doses on MI and SSA of both anatase (101) and rutile (110) phases of Titanium dioxide photoanode film.

The SSA of both phases were evaluated the following formula [6]:

$$SSA = \frac{6 \times 10^3}{\rho D_p} \tag{5}$$

where,  $\rho$  represents the nanoparticles density ( $\rho = 4.23 \text{ g}\cdot\text{cm}^{-3}$  for TiO<sub>2</sub>),  $D_p$  represents nanoparticles size.

The MI of both phases were calculated from FWHM of both anatase and rutile XRD peak by using the following formula [6]:

$$MI = \frac{FWHM_h}{FWHM_h + FWHM_p} \tag{6}$$

where,  $FWHM_h$  FWHM value obtained from peaks,  $FWHM_p$  represents measured FWHM.

It is observed from Fig. 6 that before gamma irradiation (0 kGy) of the TiO<sub>2</sub> film the SSA of anatase (101) and rutile (110) phases were found  $76.97 \text{ m}^2 \text{ g}^{-1}$  and  $44.54 \text{ m}^2 \text{ g}^{-1}$  respectively. But, at lower

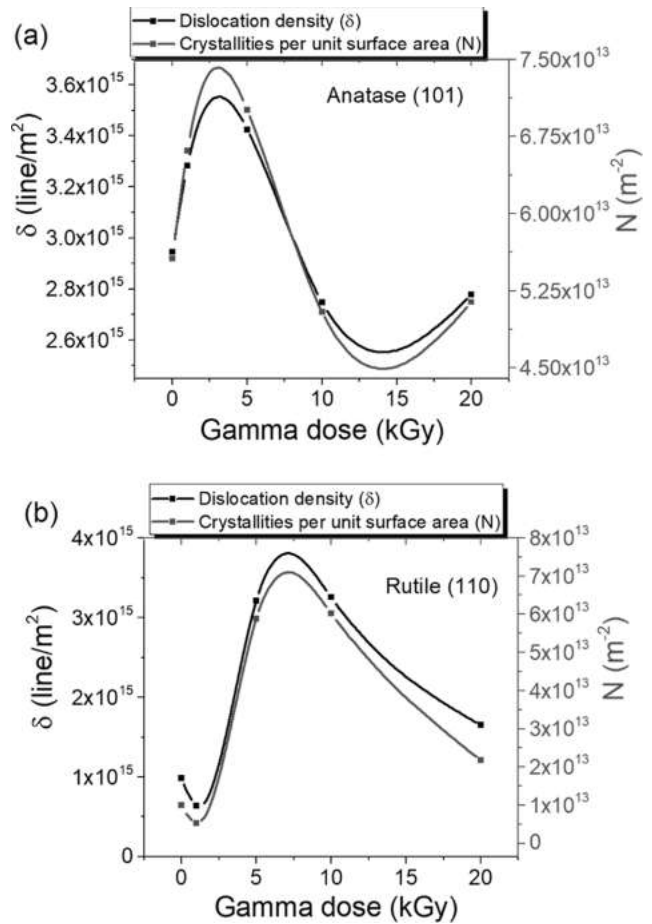


Fig. 7. Gamma doses effect on dislocation density and crystallites per unit surface area of (a) anatase (101) and (b) rutile (110) phase of TiO<sub>2</sub> (Degussa-P25) based DSSC photoanode film.

gamma radiation doses, such as 1 kGy and 5 kGy the SSA of both anatase and rutile was increased sharply. Oppositely, at higher radiation doses, such as 10 kGy and 20 kGy the SSA of both phases were decreased abruptly. Due to decreasing SSA the absorption of dye molecules may also decrease resulting lower carrier generation. Thus, decreasing SSA due to gamma irradiation becomes responsible for lowering cell efficiency of DSSC.

The MI of anatase and rutile phases were found 0.70842 and 0.80697 respectively before gamma irradiation of the TiO<sub>2</sub> film. The MI of the anatase phase was decreased at 1, 5, and 20 kGy gamma radiation doses, whereas, increased at 10 kGy dose. Besides, the MI of rutile phase was decreased at 5, 10, and 20 kGy gamma radiation doses, whereas, increased at 1 kGy dose.

Gamma irradiation effect on DD and CPSA

Fig. 7 shows the effect of different gamma radiation doses on DD ( $\delta$ ) and CPSA ( $N$ ) of both phases of TiO<sub>2</sub> thin film.

The dislocation density was calculated using the following formula [5]:

$$\delta = \frac{1}{L^2} \tag{7}$$

Also, CPSA were evaluated by the following formula [5]:

$$N = \frac{d}{L^3} \tag{8}$$

where,  $L$  represents the crystallite size for both equations above.

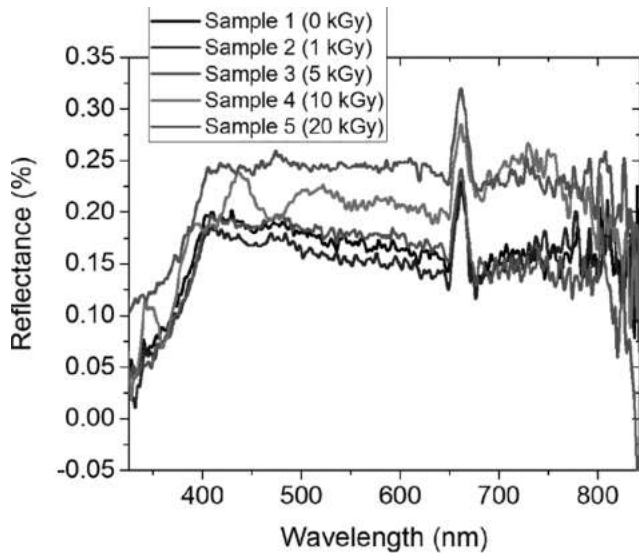


Fig. 8. Effect of gamma radiation doses on reflectance spectra of TiO<sub>2</sub> (Degussa-P25) based DSSC photoanode film.

According to the Fig. 7 that before gamma irradiation (0 kGy) of the TiO<sub>2</sub> film the dislocation density of anatase (1 0 1) and rutile (1 1 0) phase was found  $2.94 \times 10^{15}$  line/m<sup>2</sup> and  $9.86 \times 10^{14}$  line/m<sup>2</sup> respectively. Dislocation density of anatase phase was increased at lower gamma radiation doses such as 1 kGy and 5 kGy, whereas, the value decreased at higher doses such as 10 kGy and 20 kGy. Besides, the dislocation density of rutile phase was decreased sharply at 1, 5, 10, and 20 kGy gamma radiation doses.

The CPSA of anatase and rutile phase was found  $5.56 \times 10^{13}$  m<sup>-2</sup> and  $1.00 \times 10^{13}$  m<sup>-2</sup> respectively before gamma irradiation of the thin film. The CPSA of anatase was increased at lower gamma irradiation doses such as 1 and 5 kGy, whereas, the value decreased at higher gamma radiation doses such as 10 and 20 kGy. Besides, the CPSA of rutile phase were decreased abruptly at 1, 5, 10, and 20 kGy gamma radiation doses.

#### Gamma irradiation effect on optical properties

Figs. 8–10 represents the effect of gamma radiation on reflectance, transmittance, absorption, absorption depth, absorption coefficient and optical band gap energy of prepared TiO<sub>2</sub> photoanode film. The effects are discussed in detail in the following sections.

#### Gamma irradiation effect on optical reflectance

Fig. 8 showed the reflectance curve for Titanium dioxide thin film at various gamma radiation doses. According to the figure it is clear that the reflectance tends to zero below infrared range and above visible range. At infrared region the reflectance increased with increasing wavelength with minor effect of gamma irradiation. Conversely, at visible range the reflectance remains almost constant, where the irradiated sample reflected more light than the unirradiated sample. As gamma radiation is a destructive radiation it became responsible for structural disorder of the thin film which leads to change in reflectance spectra. Because of higher reflection most of the incident lights reflected from the surface of the solar cell. Thus, increase of reflectance due to gamma irradiation might affect the cell performance.

#### Gamma irradiation effect on optical transmittance

Fig. 9(a) shows the effect of  $\gamma$ -irradiation on optical transmission bands of TiO<sub>2</sub> thin film at different doses. The increased optical transmittance is found at 5 kGy. Conversely, the transmittance of the film reduced continuously with the upsurge of gamma radiation dose. This

reduction of transmittance is due to the formation of defects which is induced during irradiation. The defects accumulated and acted as color centers resulting lower light transmission through the film [40]. At higher radiation dose the production rate of defect is higher; therefore, the transmittance is lower. Lower light transmission is due to either higher absorption or reflection of incident light by the solar cell. As reflectance increased the transmittance decreased in the anodic film because of gamma irradiation. This phenomenon may be responsible for lowering solar cell performance.

#### Gamma irradiation effect on optical absorption

Fig. 9(b) shows the effect of irradiation on absorption spectra of TiO<sub>2</sub> thin film irradiated with variable gamma radiation doses. The figure shows that the light absorption decreased with increasing wavelength. At visible wavelength the irradiated samples showed lower absorption than unirradiated sample. In contrast, above visible range i.e. higher wavelength the irradiated sample showed higher absorbance than unirradiated samples.

#### Gamma irradiation effect on absorption depth

Fig. 9(c) shows the effect of  $\gamma$ -ray on absorption depth of TiO<sub>2</sub> thin films. The absorption depth of all samples was calculated following the formula [5]:

$$\delta_p = (1/\alpha) \quad (9)$$

where,  $\delta_p$  and  $\alpha$  represents absorption depth and absorption coefficient respectively. The graph represents that the absorption depth increases with increase of wavelength. At visible range the irradiated samples showed higher absorption depth than the unirradiated sample. On the other hand, above visible range the irradiated samples showed lower absorption depth than unirradiated sample. The absorption depth of a material indicates how deep a specific wavelength can penetrate before get absorbed. Increasing absorption depth indicates higher traveling time of wavelengths before absorption resulting delayed excitation formation. As gamma radiation changes the absorption depth of light in either visible or infrared region, the cell performance also changes depending on radiation doses.

#### Gamma irradiation effect on absorption coefficient

Fig. 9(d) shows the effect of  $\gamma$ -ray on absorption coefficient ( $\alpha$ ) of TiO<sub>2</sub> thin film at different gamma radiation doses. The  $\alpha$  was calculated using the following formula [5]:

$$\alpha = (2.303 A/t) \quad (10)$$

where,  $A$  and  $t$  represents the absorbance and thickness of the film respectively. According to the Fig. 9(d) it is seen that, the  $\alpha$  decreases with increase of wavelength. At visible range the unirradiated sample showed higher absorption coefficient than the irradiated samples. On the other hand, above visible range the irradiated samples showed higher absorption coefficient than unirradiated sample. The absorption coefficient of a material determines the rate of change of light intensity as it passes through a material. Lower absorption coefficient indicates lower absorption. As gamma radiation changes the absorption coefficient of light both in visible and infrared region, this phenomenon may affect the DSSC performance.

#### Gamma irradiation effect on optical band gap

Fig. 10 represents the variation in optical band gap in TiO<sub>2</sub> photoanode films at different gamma radiation doses as well as all data are tabulated in Table 4. The optical band gap values were calculated by using the following Tauc's formula [6]:

$$(\alpha h\nu)^{1/n} = A(h\nu - E_g) \quad (11)$$

Here, absorption coefficient is  $\alpha$ , energy band gap is  $E_g$ , frequency of radiation is  $\nu$ , Planck constant is  $h$  and  $A$  is a constant. As TiO<sub>2</sub> is a direct band gap material the value is considered  $n = 2$  in the formula.

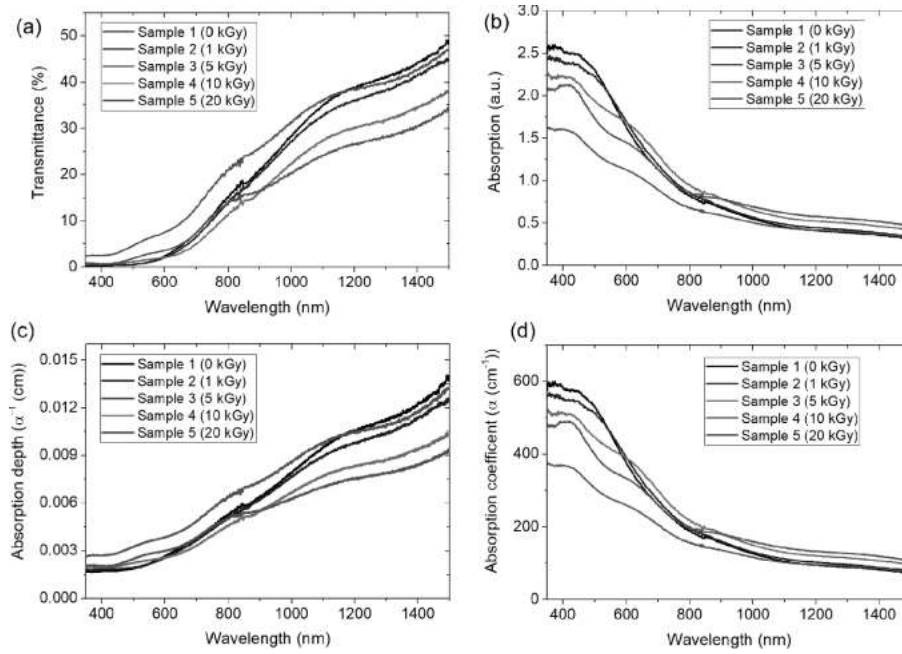


Fig. 9. Effect of gamma radiation dose on (a) transmittance spectrum, (b) absorption spectrum, (c) absorption depth, and (d) absorption coefficient of TiO<sub>2</sub> (Degussa-P25) based DSSC photoanode film.

The obtained data of  $(\alpha h\nu)^2$  was plotted against  $h\nu$  to produce graph like Fig. 10. The optical band gap of unirradiated sample (0 kGy) was found 2.80 eV. After exposure to 1, 5, 10 and 20 kGy the band gap of

respective sample was found 2.90, 2.95, 3.00 and 3.15 eV respectively. Thus, it is clear that, the optical band gap energy of TiO<sub>2</sub> thin film increases with increase of gamma radiation dose. This change in optical

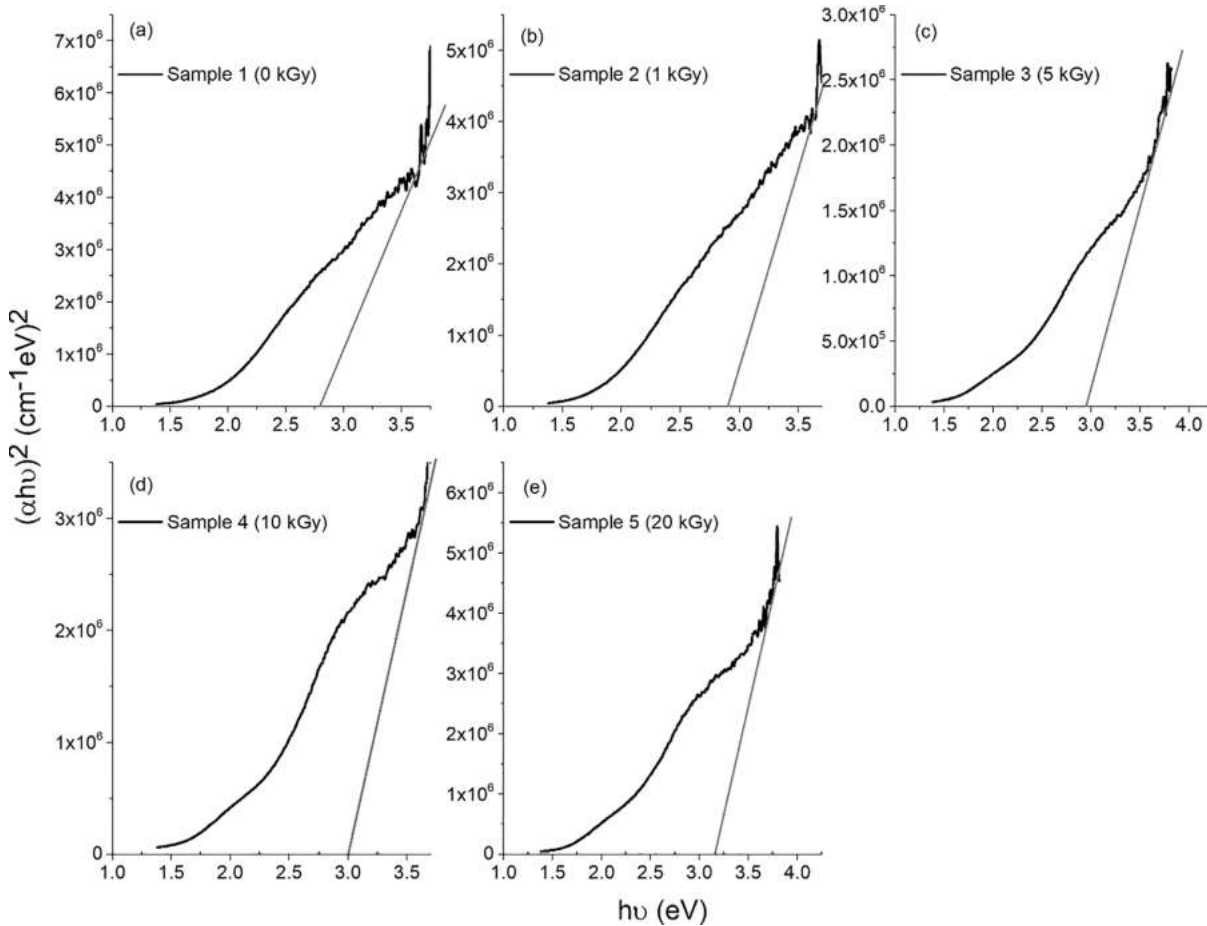


Fig. 10. Effect of gamma radiation doses on optical bandgap energy of TiO<sub>2</sub> (Degussa-P25) based DSSC photoanode film.

**Table 4**  
Effect of gamma radiation doses on optical band gap of Degussa-P25 TiO<sub>2</sub> based DSSC photoanode film.

Sample name	Radiation dose (kGy)	Optical band gap (eV)	Increase of band gap (%)
Sample 1	0	2.80	–
Sample 2	1	2.90	3.57
Sample 3	5	2.95	5.36
Sample 4	10	3.00	7.14
Sample 5	20	3.15	12.50

band gap energy in those oxide films could be attributed to quantum size effect which is due to strong interaction between the oxide nanoparticles with gamma radiation. In this case, gamma radiation effectively changed the surface microstructures, structural morphologies and particles size which led to change in optical band gap energy [41,42]. In higher band gap materials, higher energy photon is needed to produce excitons. As the gamma radiation increased the band gap of the anodic film, it requires higher energy for irradiated film to generate electron-hole pair. Thus, irradiation may cause reduction in cell performance by increasing optical band gap.

## Conclusions

In this research, the effect of  $\gamma$ -ray doses on Degussa-P25 TiO<sub>2</sub> layer of DSSC photoanode film was inspected productively. Various experiments were performed to examine the consequence of ionizing radiation on structure, morphology and optical characteristics of prepared films. The XRD presented major significant changes in MF, PC, crystallite size, strain, SSA, MI, DD, and CPSA on both phases of  $\gamma$ -irradiated TiO<sub>2</sub> film. The SEM result showed significant changes in surface morphology of the film. With the increase of gamma radiation doses both the values of mass percentage and atomic percentages decreased for Titanium and increased for oxygen in the TiO<sub>2</sub> compound. The UV–Vis result showed that with the increase of gamma radiation doses the value of both transmittance and absorption depth increased at lower wavelength and decreased at higher wavelength. On the other hand, with the increase of gamma radiation doses the value of both absorption and absorption coefficient decreased at lower wavelength and increased at higher wavelength. The optical bandgap of the sample was increased from 2.80 eV to 2.90, 2.95, 3.00 and 3.15 eV due to irradiation with 1, 5, 10 and 20 kGy gamma doses respectively. Higher transmittance and absorption coefficient is responsible for lowering the cell performance as well as higher light absorption and absorption depth helps to improve the cell performance. Therefore, due to gamma irradiation the changes in structure, morphology, composition, and optical characteristics of the nanocrystalline Titanium dioxide layer of photoanode may influence the performance of dye-sensitized solar cell.

## Author contributions

M. Khalid Hossain designed the concept and conducted the experiments. M.T. Rahman wrote the main manuscript text, while M. Khalid Hossain revised and finalized the manuscript. Remaining all co-authors reviewed the paper.

## Conflict of interest

The authors have declared no conflict of interest.

## Acknowledgement

Sample preparation were carried out at IRPT, BAEC, Bangladesh. XRD, SEM, EDS and UV–vis-NIR spectroscopy characterization were performed at IFRD, BSCIR, Bangladesh. Gamma radiation dose was

applied at GSD, IFRB, AERE, BAEC.

## References

- [1] Basher MK, Khalid Hossain M, Afaz R, Tayyaba S, Akand MAR, Rahman MT, Eman NM. Study and investigation of phosphorus doping time on emitter region for contact resistance optimization of monocrystalline silicon solar cell. *Results Phys* 2018;10:205–11. <https://doi.org/10.1016/j.rinp.2018.05.038>.
- [2] Qarony W, Hossain MI, Hossain MK, Uddin MJ, Haque A, Saad AR, et al. Efficient amorphous silicon solar cells: characterization, optimization, and optical loss analysis. *Results Phys* 2017;7:4287–93. <https://doi.org/10.1016/j.rinp.2017.09.030>.
- [3] Basher MK, Khalid Hossain M, Jalal Uddin M, Akand MAR, Shorowordi KM. Effect of the pyramidal texturization on the optical surface reflectance of monocrystalline photovoltaic silicon wafers. *Optik (Stuttg)* 2018. <https://doi.org/10.1016/j.ijleo.2018.07.116>.
- [4] Basher MK, Hossain MK, Akand MAR. Effect of surface texturization on minority carrier lifetime and photovoltaic performance of monocrystalline silicon solar cell. *Optik (Stuttg)* 2019;176:93–101. <https://doi.org/10.1016/j.ijleo.2018.09.042>.
- [5] Hossain MK, Mortuza AA, Sen SK, Basher MK, Ashraf MW, Tayyaba S, et al. A comparative study on the influence of pure anatase and degussa-P25 TiO<sub>2</sub> nano-materials on the structural and optical properties of dye sensitized solar cell (DSSC) photoanode. *Optik (Stuttg)* 2018;171:507–16. <https://doi.org/10.1016/j.ijleo.2018.05.032>.
- [6] Hossain MK, Pervez MF, Uddin MJ, Tayyaba S, Mia MNH, Bashar MS, et al. Influence of natural dye adsorption on the structural, morphological and optical properties of TiO<sub>2</sub> based photoanode of dye-sensitized solar cell. *Mater Sci* 2018;36:93–101. <https://doi.org/10.1515/msp-2017-0090>.
- [7] Hossain MK, Pervez MF, Mia MNH, Mortuza AA, Rahaman MS, Karim MR, et al. Effect of dye extracting solvents and sensitization time on photovoltaic performance of natural dye sensitized solar cells. *Results Phys* 2017;7:1516–23. <https://doi.org/10.1016/j.rinp.2017.04.011>.
- [8] Khalid Hossain M, Rahman MT, Basher MK, Manar MS, Bashar MS. Influence of thickness variation of gamma-irradiated DSSC photoanodic TiO<sub>2</sub> film on structural, morphological and optical properties. *Optik (Stuttg)* 2019;178:449–60. <https://doi.org/10.1016/j.ijleo.2018.09.170>.
- [9] Hossain MK, Pervez MF, Mia MNH, Tayyaba S, Uddin MJ, Ahamed R, et al. Annealing temperature effect on structural, morphological and optical parameters of mesoporous TiO<sub>2</sub> film photoanode for dye-sensitized solar cell application. *Mater Sci* 2018;35:868–77. <https://doi.org/10.1515/msp-2017-0082>.
- [10] Ramakrishna S, Jose R, Archana PS, Nair AS, Balamurugan R, Venugopal J, et al. Science and engineering of electrospun nanofibers for advances in clean energy, water filtration, and regenerative medicine. *J Mater Sci* 2010;45:6283–312. <https://doi.org/10.1007/s10853-010-4509-1>.
- [11] Manna L, Scher EC, Li L-S, Alivisatos AP. Epitaxial growth and photochemical annealing of graded CdS/ZnS shells on colloidal CdSe nanorods. *J Am Chem Soc* 2002;124:7136–45. <https://doi.org/10.1021/ja025946i>.
- [12] Enache-Pommer E, Boercker JE, Aydi ES. Electron transport and recombination in polycrystalline TiO<sub>2</sub> nanowire dye-sensitized solar cells. *Appl Phys Lett* 2007;91:123116. <https://doi.org/10.1063/1.2783477>.
- [13] Huang J, Wang M, Zhao J, Gao N, Li Y. Application of concentrated TiO<sub>2</sub> sols for  $\gamma$ -ray radiation dosimetry. *Appl Radiat Isot* 2001;54:475–81. [https://doi.org/10.1016/S0969-8043\(00\)00293-1](https://doi.org/10.1016/S0969-8043(00)00293-1).
- [14] Kralchevska R, Milanova M, Tsvetkov M, Dimitrov D, Todorovskiy D. Influence of gamma-irradiation on the photocatalytic activity of Degussa P25 TiO<sub>2</sub>. *J Mater Sci* 2012;47:4366–45. <https://doi.org/10.1007/s10853-012-6368-4>.
- [15] Bai Y, Mora-Seró I, De Angelis F, Bisquert J, Wang P. Titanium dioxide nanomaterials for photovoltaic applications. *Chem Rev* 2014;114:10095–130. <https://doi.org/10.1021/cr400606n>.
- [16] Bessergenev VG, Mateus MC, do Rego AMB, Hantusch M, Burkel E. An improvement of photocatalytic activity of TiO<sub>2</sub> Degussa P25 powder. *Appl Catal A Gen* 2015;500:40–50. <https://doi.org/10.1016/j.apcata.2015.05.002>.
- [17] Rogers KD, Lane DW, Painter JD, Chapman A. Structural characterization of sprayed TiO<sub>2</sub> films for extremely thin absorber layer solar cells. *Thin Solid Films* 2004;466:97–102. <https://doi.org/10.1016/j.tsf.2004.02.023>.
- [18] Hart JN, Menzies D, Cheng Y-B, Simon GP, Spiccia L. A comparison of microwave and conventional heat treatments of nanocrystalline TiO<sub>2</sub>. *Sol Energy Mater Sol Cells* 2007;91:6–16. <https://doi.org/10.1016/j.solmat.2006.06.059>.
- [19] Li W, Ni C, Lin H, Huang CP, Shah SI. Size dependence of thermal stability of TiO<sub>2</sub> nanoparticles. *J Appl Phys* 2004;96:6663–8. <https://doi.org/10.1063/1.1807520>.
- [20] Jung YH, Park K-H, Oh JS, Kim D-H, Hong CK. Effect of TiO<sub>2</sub> rutile nanorods on the photoelectrodes of dye-sensitized solar cells. *Nanoscale Res Lett* 2013;8:37. <https://doi.org/10.1186/1556-276X-8-37>.
- [21] Clough R. High-energy radiation and polymers: a review of commercial processes and emerging applications. *Nucl Instrum Methods Phys Res Sect B Beam Interact Mater Atoms* 2001;185:8–33. [https://doi.org/10.1016/S0168-583X\(01\)00966-1](https://doi.org/10.1016/S0168-583X(01)00966-1).
- [22] Ibrahim AM, Soliman LI. Effect of  $\gamma$ -irradiation on optical and electrical properties of Se<sub>1-x</sub>Te<sub>x</sub>. *Radiat Phys Chem* 1998;53:469–75. [https://doi.org/10.1016/S0969-806X\(98\)00016-4](https://doi.org/10.1016/S0969-806X(98)00016-4).
- [23] Atanassova E, Paskaleva A, Konakova R, Spassov D, Mitin V. Influence of  $\gamma$  radiation on thin Ta<sub>2</sub>O<sub>5</sub>-Si structures. *Microelectron J* 2001;32:553–62. [https://doi.org/10.1016/S0026-2692\(01\)00043-X](https://doi.org/10.1016/S0026-2692(01)00043-X).
- [24] Al-Hamdani NA HS, Al-Alawy RD. Effect of gamma irradiation on the structural and optical properties of ZnO thin films. *J Comput Eng* 2014;16:11–6.
- [25] Date H, Tomozawa H, Takamasa T, Okamoto K, Shimozuma M. Electrical conductivity of TiO<sub>2</sub> thin film on insulator induced by radiation exposure. *Jpn J Appl*

- Phys 2007;46:417–9. <https://doi.org/10.1143/JJAP.46.417>.
- [26] Banerjee D, Guin R, Das SK, Thakare SV. Effect of  $\gamma$ -dose on the crystal structure and leaching behavior of  $\text{TiO}_2$  matrix labeled with  $^{181}\text{Hf}/^{181}\text{Ta}$  tracer. *J Radioanal Nucl Chem* 2011;290:119–21. <https://doi.org/10.1007/s10967-011-1155-2>.
- [27] Samet L, March K, Stephan O, Brun N, Hosni F, Bessoua F, et al. Radiocatalytic Cu-incorporated  $\text{TiO}_2$  nano-particles for the degradation of organic species under gamma irradiation. *J Alloys Compd* 2018;743:175–86. <https://doi.org/10.1016/j.jallcom.2018.02.001>.
- [28] Reyhani A, Gholizadeh A, Vahedi V, Khanlary MR. Effect of gamma radiation on the optical and structural properties of ZnO nanowires with various diameters. *Opt Mater (Amst)* 2018;75:236–42. <https://doi.org/10.1016/j.optmat.2017.10.027>.
- [29] Wang Z, Cheng L. Gamma ray irradiation-induced variations in structure and optical properties of cerium/titanium-doped oxyfluoride transparent glass-ceramics. *Mater Res Bull* 2017;92:104–12. <https://doi.org/10.1016/j.materresbull.2017.04.010>.
- [30] Ali SM. Gamma induced effects on structural, optical and electrical properties of n- $\text{TiO}_2$ /p-Si heterojunction. *J Mater Sci Mater Electron* 2017;28:16314–20. <https://doi.org/10.1007/s10854-017-7537-7>.
- [31] Khalouie E, Jabbari I, Mirza B, Zabolian H. The effect of electron and gamma irradiation on the quality of surface and reflection of silver mirror coated by  $\text{TiO}_2$  and  $\text{Ta}_2\text{O}_5$ . *Iran J Phys Res* 2016;15:421–7. <https://doi.org/10.18869/acadpub.ijpr.15.4.421>.
- [32] Jovanović V, Samaržija-Jovanović S, Petković B, Dekić V, Marković G, Mari nović-Cincović M. Effect of  $\gamma$ -irradiation on the hydrolytic and thermal stability of micro- and nano- $\text{TiO}_2$  based urea-formaldehyde composites. *RSC Adv* 2015;5:59715–22. <https://doi.org/10.1039/C5RA10627C>.
- [33] Bello Lamo MP, Williams P, Reece P, Lumpkin GR, Sheppard LR. Study of gamma irradiation effect on commercial  $\text{TiO}_2$  photocatalyst. *Appl Radiat Isot* 2014;89:25–9. <https://doi.org/10.1016/j.apradiso.2014.02.001>.
- [34] Hossain MK, Pervez MF, Tayyaba S, Uddin MJ, Mortuza AA, Mia MNH, et al. Efficiency enhancement of natural dye sensitized solar cell by optimizing electrode fabrication parameters. *Mater Sci* 2017;35:816–23. <https://doi.org/10.1515/msp-2017-0086>.
- [35] Pervez MF, Mia MNH, Hossain S, Saha SMK, Ali MH, Sarker P, et al. Influence of total absorbed dose of gamma radiation on optical bandgap and structural properties of Mg-doped zinc oxide. *Optik (Stuttg)* 2018;162:140–50. <https://doi.org/10.1016/j.ijleo.2018.02.063>.
- [36] Mia NH, Rana SM, Pervez F, Rahman MR, Hossain K, Al Mortuza A, Basher MK, Hoq M. Preparation and spectroscopic analysis of zinc oxide nanorod thin films of different thicknesses. *Mater Sci* 2017;35:501–10. <https://doi.org/10.1515/msp-2017-0066>.
- [37] Mia MNH, Pervez MF, Hossain MK, Reefaz Rahman M, Uddin MJ, Al Mashud MA, Ghosh HK, Hoq M. Influence of Mg content on tailoring optical bandgap of Mg-doped ZnO thin film prepared by sol-gel method. *Results Phys* 2017;7:2683–91. <https://doi.org/10.1016/j.rinp.2017.07.047>.
- [38] Hoque MA, Ahmed MR, Rahman GT, Rahman MT, Islam MA, Khan MA, et al. Fabrication and comparative study of magnetic Fe and  $\alpha\text{-Fe}_2\text{O}_3$  nanoparticles dispersed hybrid polymer (PVA + Chitosan) novel nanocomposite film. *Results Phys* 2018;10:434–43. <https://doi.org/10.1016/j.rinp.2018.06.010>.
- [39] Saha SMK, Ali MH, Hossen MF, Firoz Pervez M, Mia MNH, Khalid Hossain M, et al. Structural, morphological, and optical properties of CuO thin films treated by gamma ray. 2018 Int. Conf. Comput. Commun. Chem. Mater. Electron. Eng., IEEE 2018:1–4. <https://doi.org/10.1109/IC4ME2.2018.8465649>.
- [40] Abhirami KM, Saithyamoorthy R, Asokan K. Structural, optical and electrical properties of gamma irradiated SnO thin films. *Radiat Phys Chem* 2013;91:35–9. <https://doi.org/10.1016/j.radphyschem.2013.05.030>.
- [41] Sarangi SN. Controllable growth of ZnO nanorods via electrodeposition technique: towards UV photo-detection. *J Phys D Appl Phys* 2016;49:355103. <https://doi.org/10.1088/0022-3727/49/35/355103>.
- [42] Qindeel R. Effect of gamma radiation on morphological & optical properties of ZnO nanopowder. *Results Phys* 2017;7:807–9. <https://doi.org/10.1016/j.rinp.2017.02.003>.